ELSEVIER

Contents lists available at ScienceDirect

Atmospheric Research

journal homepage: www.elsevier.com/locate/atmosres





Inferences on upward leader characteristics from measured currents

Amitabh Nag^{a,*}, Kenneth L. Cummins^{a,b}, Mathieu N. Plaisir^a, Jennifer G. Wilson^c, David E. Crawford^c, Robert G. Brown^c, R. Carl Noggle^a, Hamid K. Rassoul^a

- ^a Florida Institute of Technology, Melbourne, FL, United States of America
- b University of Arizona, Tucson, AZ, United States of America
- ^c NASA Kennedy Space Center, FL, United States of America

ARTICLE INFO

Keywords: Lightning Atmospheric electricity Upward positive leaders Upward unconnected leaders Current measurements Charge transferred to ground

ABSTRACT

We analyzed in detail currents associated with upward unconnected leaders (UULs) initiated from the Kennedy Space Center (KSC) Industrial Area Tower (IAT). Current measurements of UULs in natural lightning are relatively rare and provide important insights into the development and propagation of upward leaders. Eight UULs were initiated from the KSC-IAT between August 1, 2018 and November 15, 2019. All UULs were positive as they occurred in response to downward negative leaders that attached to ground near the tower. The KSC Mesoscale Eastern Range Lightning Information System (MERLIN) located these nearby strokes at distances ranging from 185 to 783 m from the tower, with the median being 538 m. The peak current for these strokes ranged from 13 to 69.3 kA, with the median being 26.7 kA. From the perspective of charge transferred, these UULs can be considered to be a bipolar lightning phenomenon; they transferred negative charge to ground between the inception of their current and the current-polarity reversal, following which, they effectively transferred positive charge to ground. We labeled the former time-period as the UUL development phase and the latter as the collapse phase. The median duration and charge transferred for the development phase were 789 μ s and - 6.4 mC, respectively, and for the collapse phase were 388 µs and 4.7 mC, respectively. Overall, the net charge transferred to ground by UULs was negative. During the development phase, UUL-currents consisted of faster (total durations of the order of 10 µs) impulses overlaid on slower (millisecond-scale) "background" current. The background-topeak UUL current-pulse amplitudes ranged from 3.4-289.2 A with the median being 30.1 A. The median pulse total duration and full-width at half-maximum (FWHM) were 14.1 µs and 4.9 µs, respectively. The median background-to-peak and 10-to-90% risetimes were 3.2 and 2.0 µs, respectively. Interpulse intervals ranged from 4.2-132.8 μs, with the median being 20 μs. Generally speaking, pulse amplitudes were larger, background currents were higher, and interpulse intervals were shorter at later times during UULs. It is likely that the UULs with higher background currents at later times were more closely approached by a downward leader branch versus the lower-current UULs.

1. Introduction

Measurements of lightning currents at instrumented towers are important for understanding the physics of various lightning processes, which has broad implications for lightning protection and public safety. Measurements of current in the first leader-return-stroke sequence in natural lightning can provide important insights into the characteristics of upward leaders and first return strokes. However, attachment of downward first strokes to tall, instrumented towers is relatively rare (e.g., Berger et al., 1975; Visacro et al., 2004, 2010, 2012; Takami and Okabe, 2007; Miki et al., 2019). The Industrial Area Tower (IAT) at the

Kennedy Space Center (KSC) is located in a region with flat ground experiencing lightning flash density in the range of 8 to 12 flashes/sq. km/year. A lightning current measurement system was installed on this 91.5 m tall tower supported by grounded guy wires and became operational on August 1, 2018. This relatively low-height (low enhancement) tower was selected in order to observe lightning attachment that exhibits the characteristics of natural lightning including short upward connecting and unconnected leaders in response to nearby downward leaders, natural first stroke onsets with slow-front and fast-transition characteristics, and natural first-stroke current waveforms. This is the only natural-lightning current measurement facility in the United States

E-mail address: anag@fit.edu (A. Nag).

 $^{^{\}star}$ Corresponding author.

at present.

As a downward negative leader in natural cloud-to-ground lightning approaches ground, the electric field between it and ground increases. This increasing electric field causes the development of corona, streamers, and one or more upward positive leaders are initiated from flat-ground (e.g., Cummins et al., 2018; Stolzenburg et al., 2018) or grounded objects like towers (e.g., Visacro et al., 2017a). The upward leader model by Becerra and Cooray (2006a, 2006b) predicts that the rate of change of the background field produced by a downward leader descent largely determines the conditions necessary for upward leader initiation. Upward leaders typically start several hundreds of microseconds prior to the return stroke (e.g., Visacro et al., 2017b). Upward positive leaders can then develop continuously, without distinct steps in their optical emissions (e.g., Visacro et al., 2017b). They have also been observed to move in a stepped fashion (e.g., McEachron, 1939; Biagi et al., 2011; Zhou et al., 2014; Srivastava et al., 2019; Wang et al., 2020). This is unlike downward negative leaders which appear to always propagate in a stepwise fashion. Also, in comparison to downward negative leaders, upward positive leaders are less likely to produce significant branching. Using high-speed video camera records of upward and downward leaders in a flash, Lu et al. (2013) reported that the downward leader significantly impacted the propagation direction, speed, and luminosity of the upward leader, especially just prior to attachment. This sequence leads to a return stroke when one of the initiated upward leaders connects (or attaches) with the downward leader and becomes the upward connecting leader, while the other upward leaders are called upward unconnected leaders. Positive and negative leader propagation characteristics in natural and rockettriggered lightning have been examined in various studies (e.g., Biagi et al., 2010; Biagi et al., 2011; Jiang et al., 2013; Jiang et al., 2015; Wang et al., 2016; Pu et al., 2017) and a summary is provided by Qie et al. (2019).

In this paper, we examine in detail the characteristics of measured current-waveforms of the upward unconnected leaders (UULs) initiated from the KSC-IAT in response to approaching negative leaders of strokes that attached to ground within few to several hundred meters of the tower. We also relate the UUL current waveform features to the estimated location and magnitude of the "triggering" negative cloud-toground stroke.

2. Measurement system and data

The measurement system consists of a shunt and a Rogowski coil near the base of a 6.2-m tall mast and Franklin rod installed at the top of the tower (see Fig. 1). Current from the base of the Franklin rod was brought by a down-conductor to the current measurement box at the tower top that contains the shunt and Rogowski coil. The current was measured in four separate channels, three from the shunt followed by electronic amplifiers, and one from the Rogowski coil followed by an integrator, resulting in broadband current measurements in the range of about 1 A to 200 kA. Table 1 shows the current measurement limits of each channel. Data in all channels were transmitted via fiber optic links from the tower-top to its base where they were digitized using a 12-bit oscilloscope at a rate of 25 MHz (sampling interval of 40 ns). The record-length was 2 s with a 750-ms pre-trigger. All data were GPS timestamped to allow correlation with other datasets. For the analysis in the study, UUL current waveforms recorded using the most sensitive current measurement channel (with a measurement range of 0.64 A to 600 A) were used. For portions of the waveforms when this channel was saturated (which occurred for two of our UULs), waveforms recorded using the channel with an upper limit of 24 kA were used.

Since the commencement of measurements at the tower, two downward negative flashes have attached to the tower, and were briefly described by Cummins et al. (2019). Additionally, currents from eight positive UULs initiated from the tower (due to negative return strokes in close proximity) have been recorded, which we report in this paper. The

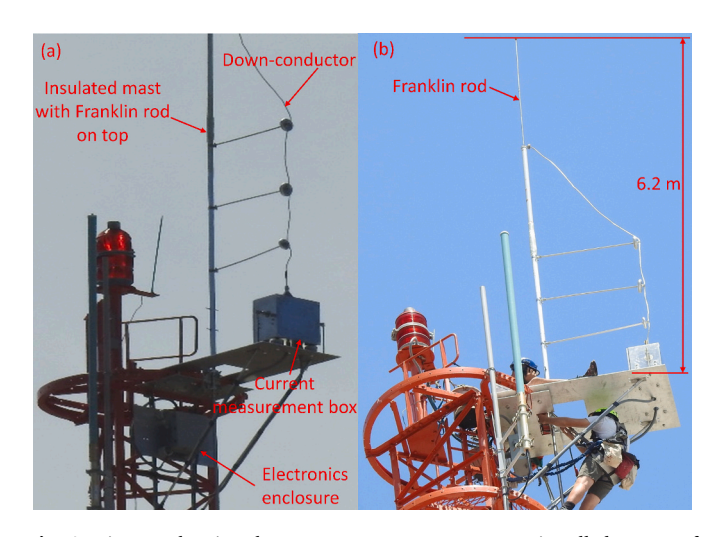


Fig. 1. Pictures showing the current measurement system installed on top of the 91.5 tall KSC Industrial Area Tower. A shunt and Rogowski coil are in the current measurement box, labeled in (a), at the base of a 6.2-m tall mast and Franklin rod, labeled in (b), installed at the top of the tower.

Table 1
Characteristics of the four current-measurement channels at the KSC IAT.

Current Measurement Device	Frequency Bandwidth	Current Saturation	RMS Noise Floor with Full Bandwidth	RMS Noise Floor with 1 MHz Bandwidth
Shunt	DC – 10 MHz	$\pm 600 \text{ A} \pm 24 \text{ kA} \pm 120 \text{ kA}$	1.73 A 33.8 A 440 A	0.64 A 12.9 A 146 A
Rogowski coil	Rogowski coil 0.05 Hz – 10 MHz		4.05 kA	1.23 kA

ground strike locations and peak currents of these nearby "triggering" strokes were estimated by the KSC Mesoscale Eastern Range Lightning Information System (MERLIN), which includes a network of ten low frequency sensors in and around KSC, similar in technology to those in the U.S. National Lightning Detection Network (NLDN). MERLIN has sensors-baselines of 10–25 km, cloud-to-ground stroke and flash detection efficiencies of 92.2% and 98.8%, respectively, a median location error of 56.5 m, and an estimated absolute peak current estimation error of 10% (Hill et al., 2016; Roeder and Saul, 2017).

3. Characteristics of UULs

3.1. Upward leader polarity and "triggering-stroke" characteristics

Fig. 2 shows the current waveforms of two UULs that occurred at the IAT. The polarity of the current waveforms shown in this figure indicate the polarity of charge effectively transferred to ground. Note here that leaders are defined to be positive or negative based on the polarity of charge distributed along their channels, while return strokes (which neutralize downward leader charge) are assigned their polarity based on the polarity of charge effectively transferred by them to ground. All eight UULs that were initiated from the KSC-IAT were positive as they occurred in response to downward negative leaders that attached to ground near the tower. All our UULs transferred negative charge to ground (by transferring positive charge into the leader channel) between the inception of their current and the current-polarity reversal, following which, they effectively transferred positive charge to ground. So, from the perspective of charge transferred to ground, UULs can be considered to be a bipolar lightning phenomenon. Throughout the period during which negative charge was being transferred, the UUL-

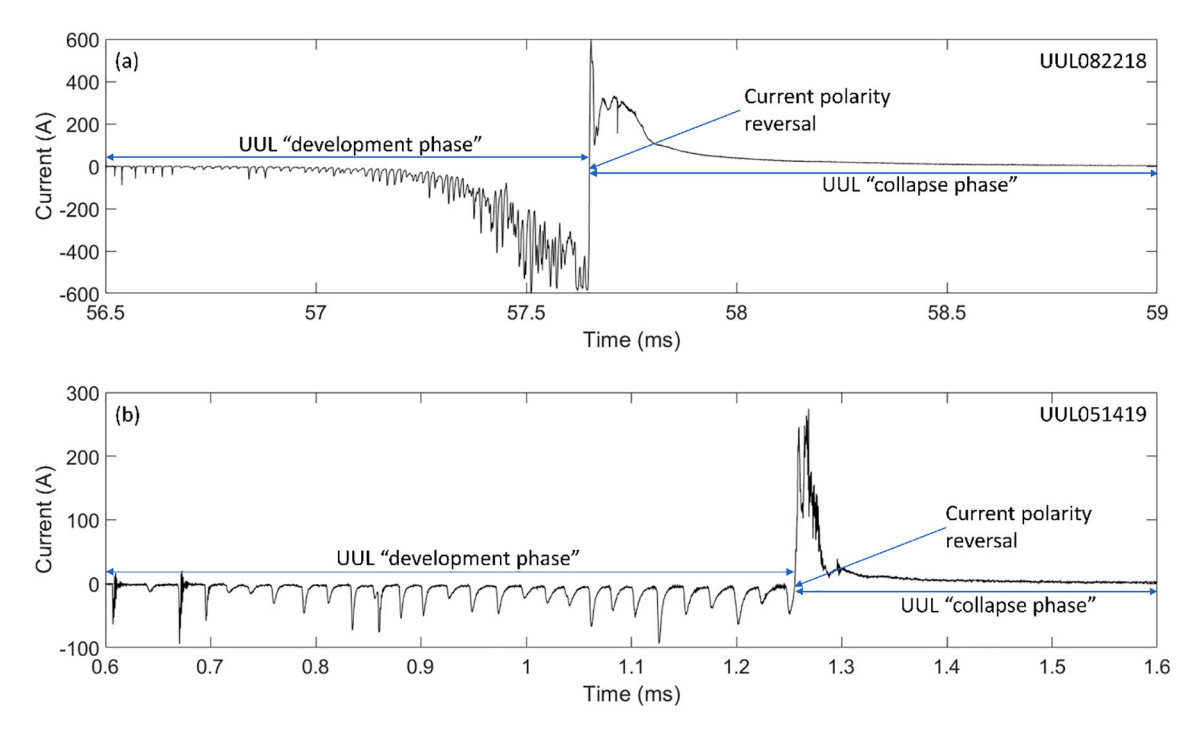


Fig. 2. The current waveforms of UULs that occurred at the KSC IAT on (a) August 22, 2018 shown on a 2.5-ms time window and (b) May 14, 2019 shown on a 1-ms time window. The polarity of the current waveforms shown in this figure indicate the polarity of charge effectively transferred to ground. These current waveforms were recorded using the most sensitive ($\pm 600 \text{ A}$) channel. The waveform in (a) was barely saturated right before and after the current polarity reversal. The MERLIN-reported distance-from-tower and peak current of the "triggering-stroke" for (a) were 393 m and -20.1 kA, respectively, and for (b) were 664 m and -26.1 kA, respectively.

currents increased with time likely accompanied by an increase in their length (see section 4 for further discussion). We have labeled this phase of UULs as their "development phase", as seen in Fig. 2. The UUL current-polarity change occurs due to reversal in the current-direction coincident with the time of ground-contact of the negative leader of the causative "triggering stroke". At this time, the direction of the electric field at ground is rapidly reversed due to the neutralization of the negative leader charge by the return stroke, resulting in the "collapse" of the UUL. We have labeled the period between the UUL current polarity reversal and the time when the current decays to zero as

the "collapse phase", as shown in Fig. 2. For our eight UULs, the MERLIN located the nearby "triggering strokes" at distances ranging from 185 to 783 m from the tower, as shown in Table 2, with the median distance being 538 m. The MERLIN-estimated peak current for these strokes ranged from -13.0 to -69.3 kA, with the median being -26.7 kA.

3.2. UUL duration, current, and charge transferred

The duration of the UUL development phase is defined as timeinterval between the inception of current in this channel and current

Table 2
Triggering stroke characteristics, and UUL duration, maximum current, and charge transferred during the development and collapse phases of the eight UULs recorded at the KSC IAT are shown. Negative signs are used to indicate negative polarity of current and charge. Range (minimum to maximum of parameter values), median, arithmetic mean (AM), and geometric mean (GM) are provided at the bottom of each column.

Flash ID	"Triggering" stroke MERLIN- reported distance from tower, km	"Triggering" stroke MERLIN- estimated peak current, kA	UUL duration, ms		UUL maximum current, A		UUL charge transfer, mC			
			Development phase	Collapse phase	Development phase	Collapse phase	Development phase	Collapse phase	Net	Total absolute
UUL082218	0.393	-20.1	1.153	1.449	-599	595	-107	63	-44	171
UUL051419	0.664	-26.1	0.686	0.344	-94	274	-7.9	5.8	-2.1	14
UUL060919	0.185	-13.0	0.919	0.484	-275	2031	-19	11	-8.1	31
UUL062319	0.250	-19.8	0.788	0.305	-56	292	-5.0	3.6	-1.4	8.6
UUL073019_003	0.645	-27.2	0.424	0.431	-69	9.2	-2.4	1.4	-1.1	3.8
UUL073019_004	0.448	-69.3	0.791	0.900	-333	1035	-22	15	-6.9	37
UUL110519_002	0.629	-57.0	0.116	0.086	-82^{a}	42	-0.5	0.4	-0.1	0.9
UUL110519_006	0.783	-54.2	0.877	0.215	-41	58	-4.0	2.2	-1.8	6.3
Range	0.185 to 0.782	-13.0 to -69.3	0.116 to 1.153	0.086 to 1.449	-41 to -599	9.2 to 2031	-0.5 to -107	0.4 to 63	-0.1 to -43.8	0.9 to 171
AM	0.500	-35.8	0.719	0.527	-194	542	-21	13	-8.1	34
Median	0.538	-26.7	0.789	0.388	-88	283	-6.4	4.7	-2.0	11
GM	0.451	-30.7^{b}	0.612	0.389	$-127^{\rm b}$	197	-7.4 ^b	4.8	-2.4^{b}	12

^a The background current during this UUL's development phase was nearly zero (below the measurement threshold of our most sensitive channel). All UUL pulses were distorted to some degree (see sections 3.2 and 3.3 for further discussion). The maximum current value shown is the peak current of such a distorted pulse and should be treated as an overestimate.

b The absolute values of parameters are taken to compute the geometric mean. The negative sign indicates effective transfer of negative charge to ground.

polarity-reversal (see Fig. 2). We defined the inception of UUL current as the start time of the first pulse in a series of microsecond-scale current pulses occurring at somewhat regular intervals during the UUL development phase. As shown in Table 2, the development-phase durations for our eight UULs ranged from 116 µs to 1.15 ms, with the median being $789 \mu s$. The duration of the UUL collapse phase is defined as timeinterval between the current polarity-reversal and when the current in the measurement channel decays to below our measurement threshold (of less than 1 A, see Table 1). These durations ranged from 86 μs to 1.45 ms, with the median being $388 \mu s$. The highest values of currents during the two phases ranged from -41 to -599 A and from 9.2 to 2031 A, respectively, with the medians being -88 and 283 A, respectively. Note that while measuring these maximum currents we ignored the peaks of sharply rising pulses with durations of about 1–2 µs or less. These shortduration pulses (for example, the first and third pulses in Fig. 2b) appeared to be faster than the frequency-response upper-limit of our measurement system (due to which their waveforms were distorted) and occurred during both phases of UULs, but mostly at the inception of the UUL currents. The exact reason for their appearance is currently unknown but could be due to corona emissions from our Franklin rod or induced effects of the approaching negative leader on the tower and our measurement system. We also ignored such pulses in our analysis in section 3.3. Charge transferred during the UUL development and collapse phases were computed by digitally integrating the current waveforms over appropriate times. Negative charge transferred to ground during the development phase ranged from -0.5 to -107 mC, with the median being -6.4 mC. During the collapse phase, positive charge ranging from 0.4 to 63 mC was effectively transferred to ground, with the median being 4.7 mC. So, the net charge transferred to ground by the UULs ranged from -0.1 to -43.8 mC, with the median being -2.0mC. Also, the total absolute (magnitude of) charge transferred by UULs ranged from 0.9 to 171 mC, with the median being 11 mC.

Fig. 3a shows the scatter plot of the MERLIN-reported peak currents for "triggering-strokes" versus the distance from the tower of the strokes' MERLIN-estimated ground-attachment points for the eight UULs. In general, triggering-strokes with higher peak currents attached to ground at farther distances from the tower. Fig. 3b and c show the scatter plots of the charge-transferred by UULs versus their duration during the development and collapse phases, respectively. While more data are needed to quantify a relationship between these two parameters, it appears that charge transferred increases non-linearly with increasing duration, at least during the UUL development phase.

3.3. Characteristics of microsecond-scale UUL pulses

We examined in detail the characteristics of the microsecond-scale current pulses that occurred during the development phase of the eight UULs recorded at the KSC IAT. These pulses result in the injection of positive charge into the upward leaders effectively transferring negative charge to ground (see the section 4 for discussion on reasons for their occurrence). Table 3 shows the characteristics of these pulses for seven of these eight UULs. One UUL (UUL110519_002 in Table 2) was associated with a (MERLIN-estimated) -57 kA triggering stroke striking ground at a distance of 629 m from the tower. Its current waveform contained only six microsecond-scale pulses (all with somewhat distorted waveforms, see section 3.2) and it is not included in Table 3. As seen in Fig. 2a, UUL-currents typically consist of faster (total durations of the order of 10 µs) impulses overlaid on slower (millisecond-scale) "background" current. Fig. 4a-f show histograms of the characteristics of pulses occurring during the seven UULs. Note that for UUL082218 (waveform shown in Fig. 2a), UUL060919, and UUL073019_004, starting 438, 202, and 95 µs prior to current polarity reversal, respectively, the interpulse intervals were short enough that the successive pulses overlapped and some pulse features could not be distinctly measured. The total duration, full-width at half-maximum (FWHM), and risetimes could be measured for 179 pulses occurring in the seven UULs shown in

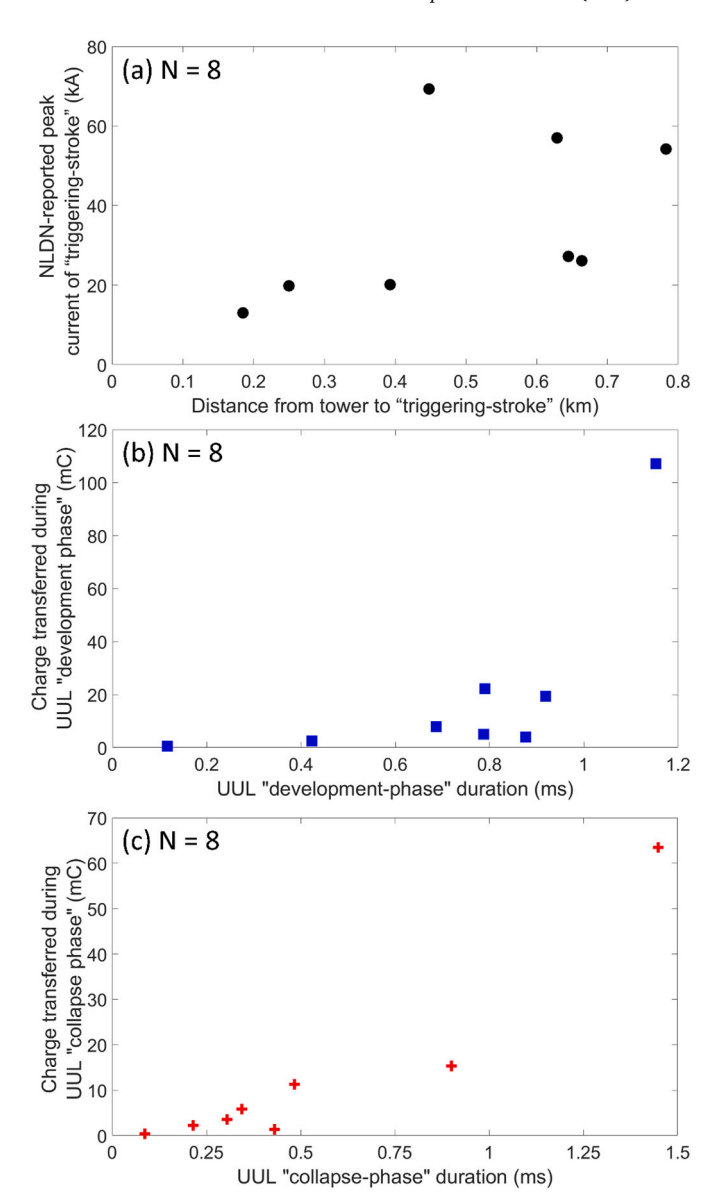


Fig. 3. Scatter plots for eight UULs in our dataset showing (a) MERLIN-reported peak currents for "triggering-strokes" versus the distance from the tower of the strokes' MERLIN-estimated ground-attachment points, (b) charge-transferred by UULs during their development phase versus their development-phase duration, and (c) charge-transferred by UULs during their collapse phase versus their collapse-phase duration. Note that negative (blue squares in (b)) and positive (red plusses in (c)) charges were transferred to ground during the UUL development and collapse phases, respectively; only the charge magnitudes are shown in (b) and (c).

Table 2. The median pulse total duration and FWHM were 14.1 μs and 4.9 μs , respectively. The median background-to-peak and 10-to-90% risetimes were 3.2 and 2.0 μs , respectively. The median background-to-peak pulse amplitudes for 223 pulses ranged from -3.4 to -289.2 A with the median being -30.1 A. Note that we measured the pulse amplitudes relative to the background current-level at the start of each pulse rather than the zero current-level in order to separately examine the impulsive and slowly-varying components of UUL current. The 216 interpulse intervals ranged from 4.2–132.8 μs , with the median being 20 μs .

The charge injected during each UUL pulse was defined as the charge transferred between its start and end times. Fig. 5a shows the histogram of the pulse charge magnitude for 179 pulses in the seven UULs listed in Table 3. The pulse charge magnitude ranges from 29.7 to 1140 μ C with

Table 3
Summary of characteristics of microsecond-scale current pulses in seven of our eight recorded UULs. Note that these pulses injected positive charge into the UULs, therefore, effectively transferring negative charge to ground. One UUL (UUL110519_002 in Table 2, see also its footnote a) contained only six microsecond-scale pulses and is not included in this table. The numbers in brackets in each cell indicates the number of pulses for which the statistics are provided.

Flash ID		Total duration, μs	Full-width at half maximum, µs	Background-to-peak risetime, μs	10-to-90% risetime, μs	Background-to-peak pulse amplitude, A	Interpulse interval, μs	Pulse charge magnitude, μC
UUL082218	Median (Sample size)	13.2 (N = 32)	4.5 (N = 32)	2.7 (N = 32)	1.7 (N = 32)	47.1 (<i>N</i> = 58)	16.5 (<i>N</i> = 57)	176 (N = 32)
	Range	5.3-21.0	1.4-7.6	0.8-12.3	0.5-10.6	7.9-289.2	4.2-30.8	37.5-646
UUL051419	Median (Sample size)	17.1 $(N = 23)$	4.5 (N = 23)	3.8 (N = 23)	2.2 (N = 23)	60.2 (N = 23)	22.7 (N = 22)	267 (N = 23)
	Range	11.3-21.7	2.2-6.9	2.0-8.2	1.1-5.6	89.9-46.5	20.3-28.6	109-519
UUL060919	Median (Sample size)	12.6 (N = 35)	5.3 (N = 35)	2.8 (N = 35)	2.1 (N = 35)	22.1 (N = 47)	15.7 $(N = 46)$	124 (N = 35)
	Range	5.7-21.1	1.2-13.6	1.0-11.6	0.4-10.6	6.3-208.9	20.9-36.7	29.7-497
UUL062319	Median (Sample size)	16.6 (N = 22)	7.9 (N = 22)	3.7 (N = 22)	2.7 (N = 22)	15.2 (N = 22)	26.4 (N = 21)	169 (N = 22)
	Range	5.8-25.7	1.3-19.2	1.9-11.4	1.2-7.3	7.3-56.4	20.0-43.4	70.5-288
UUL073019_003	Median (Sample size)	11.4 (N = 17)	3.6 (N = 17)	2.2 (N = 17)	1.2 (N = 17)	22.1 (N = 17)	19.9 $(N=16)$	108 (N = 17)
	Range	5.7-16.7	0.8-8.5	0.8-5.3	0.4-3.9	8.7-69.1	16.1-22.2	48.0-173
UUL073019_004	Median (Sample size)	12.4 (N = 30)	3.5 (N = 30)	2.6 (N = 30)	1.5 (N = 30)	61.1 (N = 36)	20.8 (N = 35)	261 (N = 30)
	Range	5.4-22.4	0.7-13.6	0.6-5.9	0.3-3.4	6.8-266.2	6.2-28.8	47.3-1140
UUL110519_006	Median (Sample size)	17.0 (N = 20)	8.2 (N = 20)	4.4 (N = 20)	3.4 (N = 20)	10.3 (N = 20)	23.6 (N = 19)	97.9 (N = 20)
	Range	7.2-34.0	2.0-22.2	1.5-18.0	1.1-17.5	3.4-39.7	17.1-132.8	36.3-207
All	Median (Sample size)	14.1 (N = 179)	4.9 (N = 179)	3.2 (N = 179)	2.0 (N = 179)	30.1 (N = 223)	$20.0 \ (N=216)$	157 (N = 179)
	Range	5.3–34.0	0.7-22.2	0.6-18.0	0.3–17.5	3.4–289.2	4.2–132.8	29.7–1140

the median being 157 μ C. Fig. 5b shows the scatter plot of pulse charge magnitude versus time from first pulse peak, color-coded by flash ID. Generally speaking, for all our UULs the pulse charge increases (at varying rates) for pulses occurring later in the UUL. This increase is most noticeable for UUL073019_004 (yellow colored dots in Fig. 5b) and the least apparent for UUL 110519_006 (dark green colored dots).

4. UUL parameter inter-relationships, inferences, and discussion

Fig. 6 shows scatter plots of various parameters of the seven UULs listed in Table 3, color-coded by flash ID. Fig. 6(a), (c), and (e) show, respectively, the absolute background current amplitude, absolute background-to-peak pulse-amplitude, and interpulse interval versus time from first pulse peak. It appears that for $500 \mu s$ or so after the first pulse peak the background current, pulse-amplitudes, and interpulse intervals did not change remarkably. Six out of the seven UULs included in the scatter plots lasted longer than $500 \, \mu s$. As can be clearly seen from Fig. 7a, the absolute background current was less than about 13 A up to $500 \mu s$, after which three of the six continuing UULs exhibited steadily increasing currents. For these three UULs (UUL082218, UUL060919, and UUL073019_004 in Table 2 and indicated by blue, light green, and yellow colored dots, respectively, in Figs. 6 and 7) the triggering strokes attached to ground at MERLIN-reported distances of 393, 184, and 448 m from the tower (see Table 2), respectively, and had MERLIN-estimated peak currents of -20.1, -13.0, and -69.3 kA, respectively. The median absolute background current before and after 500 µs for these three UULs were 2.7 and 28 A, respectively, while they were 2.1 and 4.3 A, respectively, for the other three UULs lasting longer than 500 µs from first pulse peak. The latter three UULs (UUL051419, UUL062319, and UUL110519 006 indicated by red, black, and dark green dots, respectively, in Figs. 6 and 7) therefore, did not display a large (order of magnitude) increase in the median background current. The triggering strokes for these attached to ground at distances of 664, 250, and 783 m from the tower, respectively, with their estimated-peak currents being -26.1, -19.8, and -54.2 kA, respectively. The pulse-amplitudes for all six UULs lasting longer than 500 µs were less than 100 A up to 500 µs from first-pulse peak, with the exception of one pulse, as seen in Fig. 7b. For the three higher-background-current UULs, the median pulseamplitudes before and after that time were 23.5 and 78.3 A, respectively. The before/after medians for the three lower-background-current $\,$ UULs were 20.7 and 9.1 A, respectively. Finally, the interpulse intervals showed a small decrease starting at around 500 μs after the first pulse peak (see Fig. 7c) for the three higher-current UULs, with the median interpulse intervals being 19.4 and 14.6 µs before and after that time, respectively. For the three lower-background-current UULs, the medians were 24.6 and 22.7 µs, respectively.

The UUL background current amplitude is likely related to the length of developing upward leader as it clearly depends upon the duration of the upward leader (see Fig. 6a). These parameters (UUL background current amplitude, length, and duration) are determined by the local electric field due to the approaching downward leader. If the upward leader length increases with time, the background current level increases. The significant increases in background current at later times during the three UULs (discussed above) likely signify that these UULs developed to be of significant lengths (perhaps several tens to 100 m). It is likely that in each of these cases a negative downward leader branch and the UUL approached each other closely, perhaps getting within 100 m or so of each other, just prior to another branch of the downward leader attaching to ground via a UCL in the tower's proximity. When the distance between the tip of the UUL and the most proximate downward-leader branch-tip stops decreasing the electric field between them is expected to not increase with time, which will likely cause the upward leader to stop developing further (no significant increase in length and current). So, the three UULs for which the background current did not increase significantly at later times (discussed above), were likely relatively stagnant (from the perspective of their length) upward leaders. In fact, this may also be true for two additional UULs, one of whose development phase lasted for 424 µs (UUL073019_003 shown using pink dots in Figs. 6 and 7) and the other whose development phase lasted for 116 µs (UUL110519_002 in Table 2) and did not contain a significant number of UUL-current pulses. High-speed video observations of UULs in conjunction with their current measurements are needed to confirm these speculations.

No clear relationship between UUL background currents and the background-to-peak pulse amplitudes were apparent as can be seen from Fig. 6b. This could be related to step pulses being produced by at least two different mechanisms – displacement currents from the approaching negative leader (see below) and inherent positive leader stepping. This is perhaps also apparent from the larger scatter (variation) in the pulse amplitudes (Fig. 6c) versus in the background currents (Fig. 6a) at later times during the UULs.

Interpulse intervals were shorter for pulses with larger peak amplitudes and also when the UUL background current was higher (see Fig. 6d and f). This is consistent with the observations that pulse amplitudes are larger, background currents are higher, and interpulse intervals are shorter at later times during UULs, when the local electric field due to the approaching negative leader is higher.

The (microsecond-scale) current pulses occurring during the development phase of UULs effectively result in the upward leader being supplied with positive charge from ground. Visacro et al. (2017b)

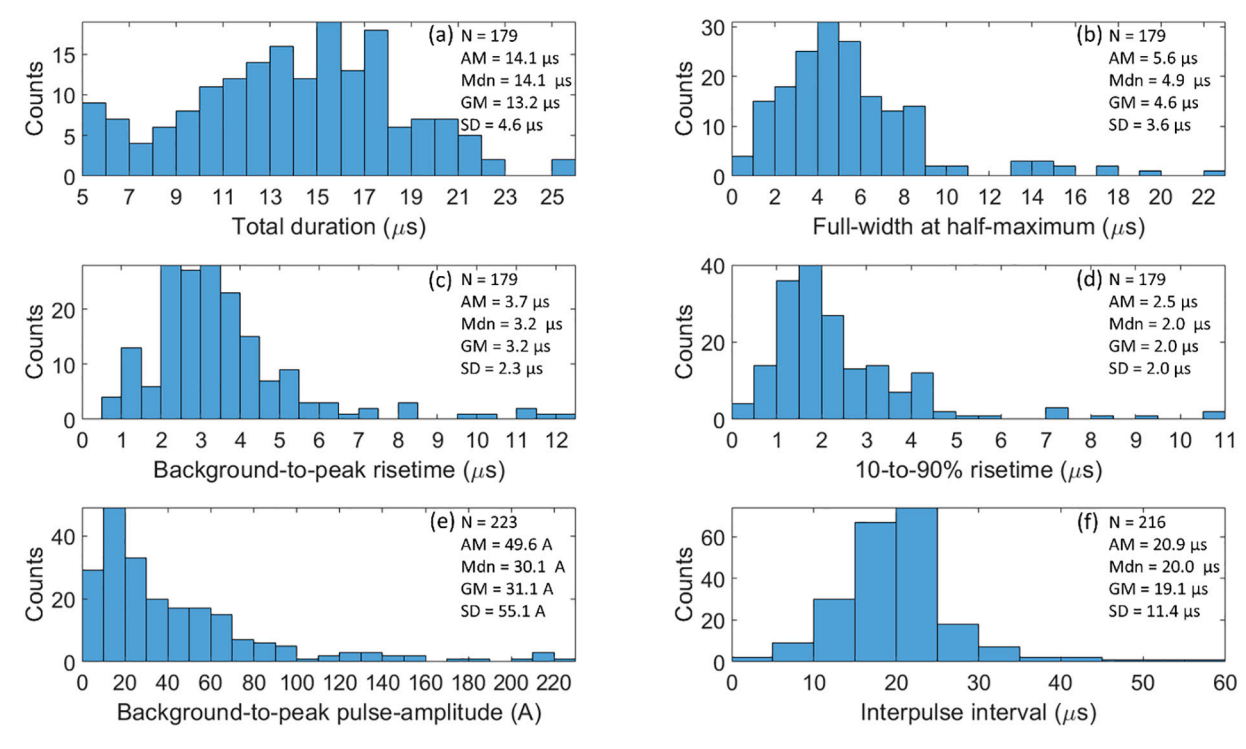


Fig. 4. Histograms showing the (a) total duration, (b) full-width at half-maximum, (c) background-to-peak risetime, (d) 10-to-90% risetime, (e) absolute background-to-peak pulse amplitude, and (f) interpulse intervals for current pulses occurring during the seven UULs listed in Table 3. An additionally recorded UUL (UUL110519_002 in Table 2, see also its footnote a) contained only six pulses and these are not included in the histograms. Note that the horizontal axes upper limits in (a), (c), (d), (e), and (f) are truncated at less than the maximum values of the respective parameters. Only 1 pulse each in (a), (c), and (d), and 5 and 2 pulses, in (e) and (f), respectively, had parameter-values greater than the histogram horizontal axes limits. Statistics shown are sample size (N), arithmetic mean (AM), median (Mdn), geometric mean (GM), and standard deviation (SD). The corresponding maximum and minimum values are shown in Table 3.

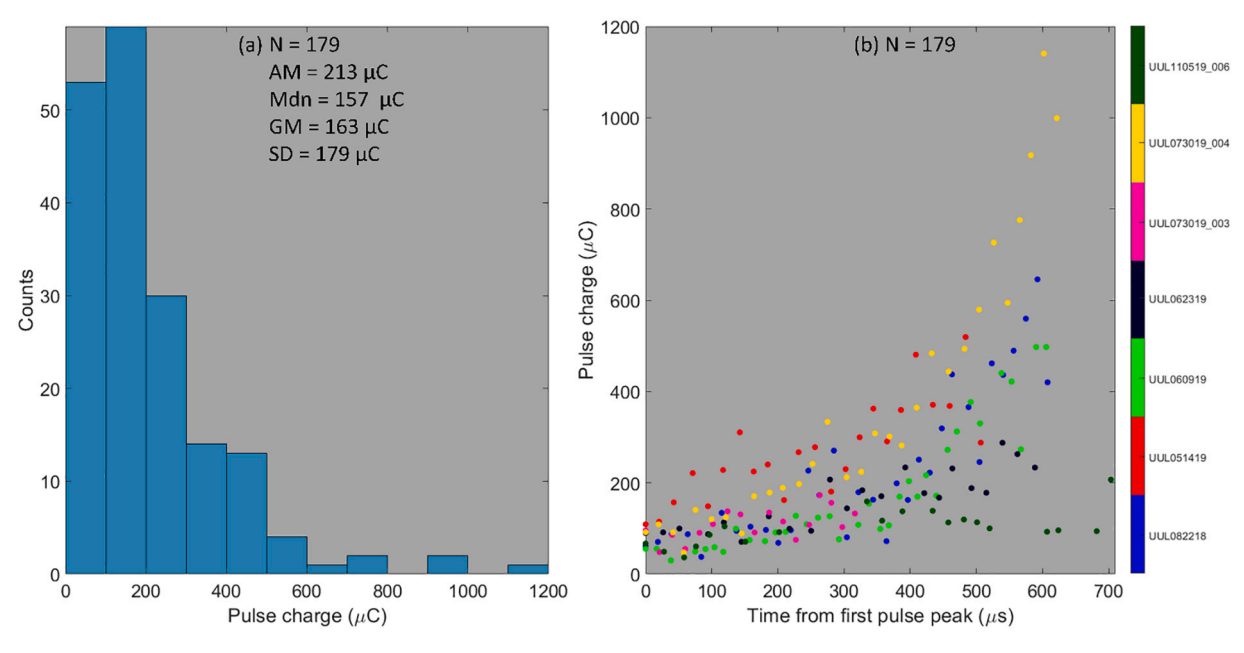


Fig. 5. (a) Histogram of the magnitude of pulse charge (charge injected by each UUL pulse) and (b) scatter plot showing pulse-charge magnitude versus time from first pulse peak for 179 pulses in the seven UULs listed in Table 3, color-coded by flash ID. Note that these pulses injected positive charge into the UULs, therefore, effectively transferring negative charge to ground. Statistics shown in (a) are sample size (N), arithmetic mean (AM), median (Mdn), geometric mean (GM), and standard deviation (SD). The corresponding maximum and minimum values are shown in Table 3.

hypothesized that the "superimposed unipolar pulses of current" occurring during the UUL development-phase are induced by the steps of the negative leader approaching ground based on the time-synchrony of these features, and on Schoene et al.'s (2008) measurements of

induced unipolar current pulses along a vertical grounded conductor before a nearby negative flash. Downward negative leader stepping produces electric-field pulses (displacement current) that couple with the upward leader. Thus, features of UUL current pulses such as

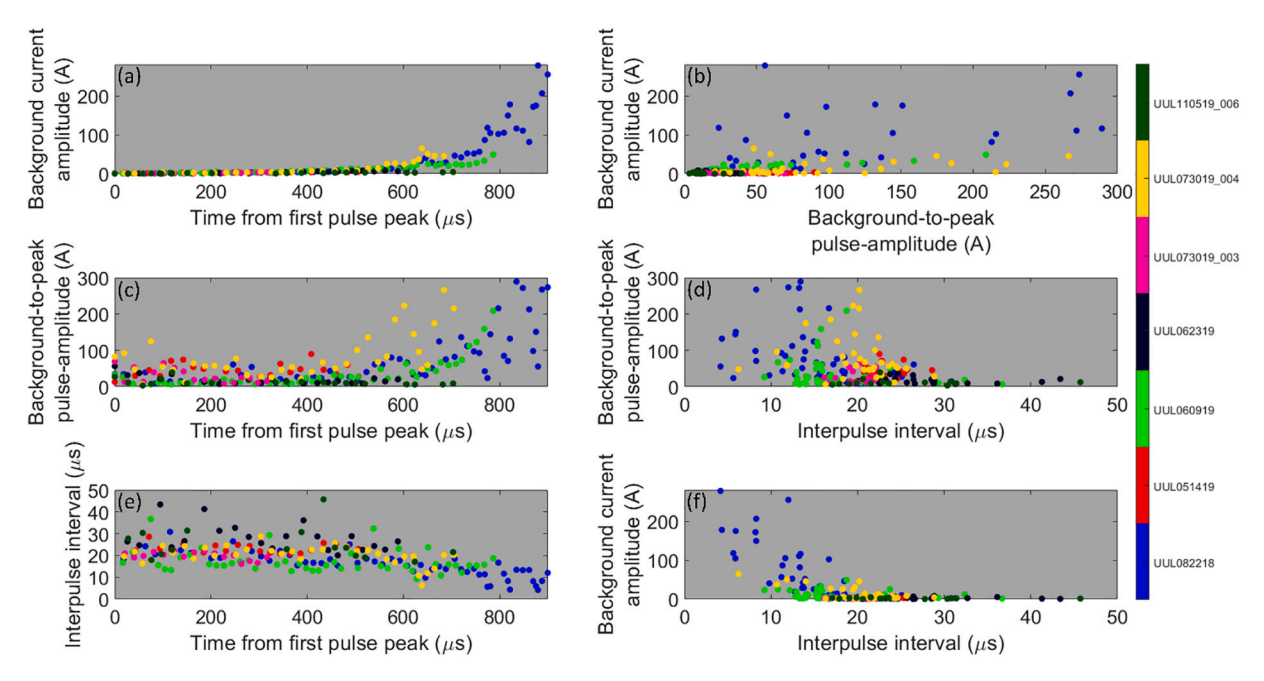


Fig. 6. Scatter plots of the (a) absolute background current amplitude versus time from first pulse peak, (b) background current amplitude versus background-to-peak pulse-amplitude, (c) background-to-peak pulse-amplitude versus time from first pulse peak, (d) background-to-peak pulse-amplitude versus interpulse interval, (e) interpulse interval versus time from first pulse peak, and (f) background current amplitude versus interpulse interval for the seven UULs listed in Table 3, color-coded by flash ID. Absolute values of the currents are shown. Note that the horizontal axes in (d) and (f) and vertical axis in (e) were truncated at 50 μs; only 4 interpulse intervals were greater than this value. The color bar to the right indicates the flash IDs for which the data are presented in the scatter plots.

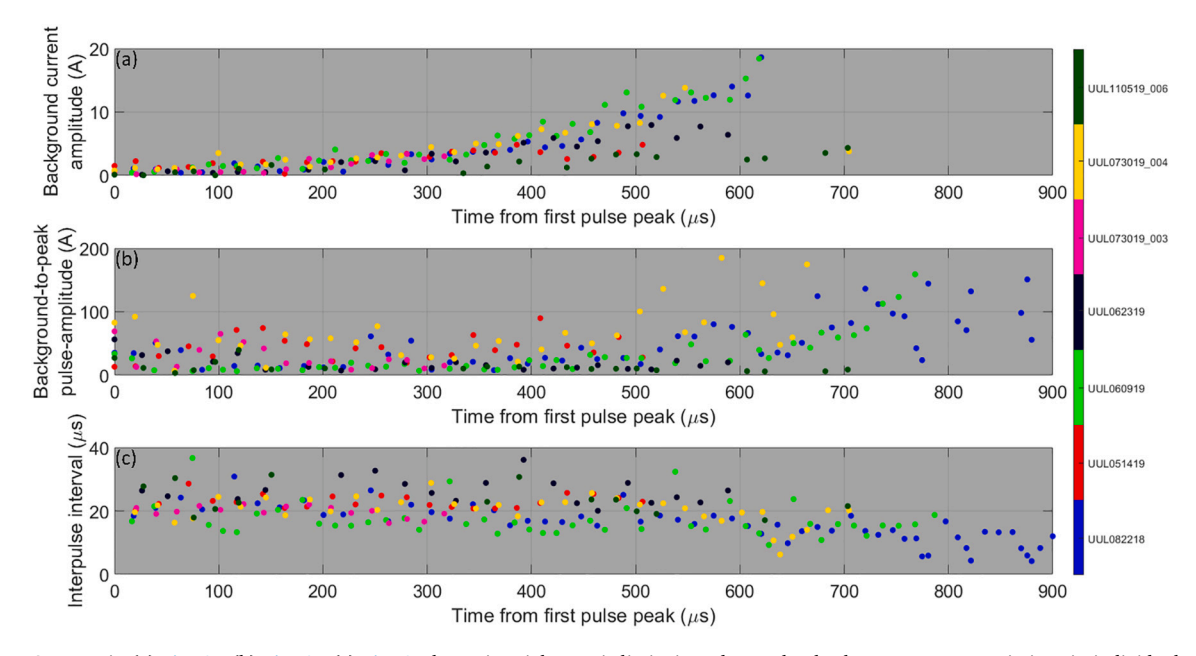


Fig. 7. Same as in (a) Fig. 6a, (b) Fig. 6c, (c) Fig. 6e, but using tighter axis limits in order to clearly show parameter variations in individual UULs.

amplitude, injected charge, risetimes, and interpulse interval are likely influenced by downward leader channel geometry and branching, characteristics of downward leader steps, distance between the upward and downward leaders, as well as UUL channel characteristics. This is consistent with our observations (discussed above) that higher current UULs show an increase in pulse amplitudes and decrease in interpulse intervals at later stages compared to lower current UULs, as well as with our hypothesis that the higher-current (at later times) UULs were more closely approached by a downward leader branch versus the lower-current UULs which remained relatively stagnant. Note that, interpulse intervals of cloud-to-ground negative stepped-leader electric

pulses are shorter and their amplitudes are larger at later stages of the negative downward leader as it approaches ground (see for example, Rakov and Uman, 2003, pp. 132–135). Krider et al. (1977) inferred that the minimum charge involved in the formation of a downward leader step is 1–4 mC, which is about an order of magnitude larger than the median UUL pulse charge of 157 μC and comparable to the maximum UUL pulse charge of 1.14 mC in our dataset (see Table 3). We do not have sufficient information to evaluate the contribution of inherent stepping in upward positive leaders to the current pulses that we report here.

Visacro et al. (2010) examined the characteristics of 75 current

pulses in two positive UULs measured at the Morro do Cachimbo Station in Brazil, and reported the arithmetic mean (AM) pulse amplitude to be 86 A, which is larger than the AM background-to-peak pulse amplitude of 49.6 A for 223 pulses in our dataset (see Fig. 4e). This is likely because we measured the peak pulse amplitudes from the background currentlevel rather than from the zero current-level (as noted in the section 3.3), as apparently done by Visacro et al. (2010). The AM pulse duration, risetime, and interpulse interval reported by Visacro et al. were 8.0, 4.9, and 68.9 µs, respectively. In our dataset (see Fig. 4a, c, and f), they were 14.1 (N = 179), 3.7 (N = 179), and 20.9 μ s (N = 216), respectively. Our AM pulse durations are 1.8 times longer and interpulse intervals 3.3 times shorter than those reported by Visacro et al. A possible reason for the observed difference in interpulse intervals could be more profuse branching in downward leaders at the KSC IAT versus at the Morro do Cachimbo Station (MCS) where Visacro et al.'s measurements were performed. As developing downward leader branches do not step synchronously, such stepping would induce current pulses in UULs at different times tending to diminish the UUL interpulse intervals. We do not have sufficient evidence at present to confirm this speculation. Finally, for both their UULs, Visacro et al. reported that the background currents gradually rose from zero but retained a relatively steady value until the current polarity reversal when the upward leader collapsed (see Visacro et al.'s Fig. 8). The triggering strokes for these UULs occurred at distances of a few hundred meters and about 2 km from the tower. These two UULs are therefore similar (at least from the perspective of their current waveforms) to our UUL051419 shown in Fig. 2b. In fact, five of our eight UULs were of this low-background-current type, while for the other three the background currents grew to relatively high values just prior to polarity reversal (as discussed in the preceding two paragraphs). Note that the MCS consists of a 60 m high insulated mast on top of a mountain 1430 m above sea level (Visacro et al., 2010). As noted by an anonymous reviewer, it is likely that this mast has a larger attractive radius than the KSC IAT (our tower) which is a 91.5-m tall, grounded tower located at sea level, supported by conducting guy-wires, and with a 6.2-m high mast and Franklin rod on top. This results in cloud-toground strokes being able to terminate relatively close (as close as 184 m, see Fig. 3a) to the KSC IAT. Such close-to-the-tower strikes would likely be "prevented" by the larger attractive radius of the MCS. This is consistent with our hypothesis that the higher-background-current UULs observed by us were due to closer approach by downward leaders.

The unconnected leader collapses due to the rapid reversal of the electric field occurring at the time of the return stroke. Thus, the displacement current associated with the return stroke electric field change likely influences the collapse-phase UUL currents. For two ULLs in our dataset the collapse phase maximum current was greater than 1 kA; they were 2031 A and 1035 A, which were significantly higher than their respective development phase maximum currents of $-275\,\mathrm{A}$ and $-333\,\mathrm{A}$. Interestingly, the $-13\,\mathrm{kA}$ triggering stroke for the first of these UULs attached to ground at 185 m, which is the shortest distance-fromtower in our dataset. Also, the triggering stroke for the second UUL attached to ground at 448 m from the tower and had an estimated peak current of $-69.3\,\mathrm{kA}$, which is the highest triggering-stroke peak current in our dataset.

5. Summary

The Industrial Area Tower at the Kennedy Space Center is located in a region with a lightning flash density of 8 to 12 flashes/sq. km/year. A lightning current measurement system was installed at the IAT in July-August 2018. The measurement system was operational on August 1, 2018. The measurement system consists of a shunt and a Rogowski coil near the base of a 6.2-m tall mast and Franklin rod installed at the top of the tower. Since the commencement of measurements at the tower, two downward negative flashes have attached to the tower. Additionally, currents from eight upward unconnected leaders due to nearby negative cloud-to-ground triggering strokes were measured. These strokes were

located by the KSC MERLIN at distances ranging from 185 to 783 m from the tower, with the median being 538 m. The peak current for these strokes ranged from 13 to 69.3 kA, with the median being 26.7 kA. In this study we examined in detail the characteristics of the measured current waveforms for these eight UULs.

From the perspective of charge transferred to ground, UULs can be considered to be a bipolar lightning phenomenon. All our UULs initially transferred negative charge to ground between the inception of their current and the current-polarity reversal. We labeled this time-period as the UUL development phase. Following this, the UULs effectively transferred positive charge to ground, which we labeled as the UUL collapse phase. The polarity change occurs due to reversal in the UUL current-direction near the time of ground-contact of the negative leader of the causative triggering stroke.

The durations of the development phase of the eight UULs ranged from 116 µs to 1.15 ms, with the median being 789 µs. Negative charge transferred to ground during this phase ranged from 0.5 to 107 mC, with the median being 6.4 mC. The collapse-phase durations ranged from 86 μs to 1.45 ms, with the median being 388 μs , during which 0.4 to 63 mC of positive charge was transferred to ground with the median being 4.7 mC. UUL-currents consisted of faster (total durations of the order of 10 μs) impulses overlaid on slower (millisecond-scale) "background" current. These impulses injected positive charge into the UULs, therefore, effectively transferring negative charge to ground. The faster current pulses are likely dominantly influenced by the electric field changes from stepping in the downward leader. The background-to-peak UUL current-pulse amplitudes for 223 pulses ranged from 3.4-289.2 A with the median being 30.1 A. Interpulse intervals ranged from 4.2–132.8 μs, with the median being 20 µs. The median total pulse duration and FWHM for 179 of these pulses were 14.1 μs and 4.9 μs , respectively. The median background-to-peak and 10-to-90% risetimes were 3.2 and 2.0 μs, respectively. Magnitude of pulse charge during the development phase ranged from 29.7–1140 $\mu\text{C},$ with the median being 157 $\mu\text{C}.$ We do not have sufficient information to evaluate the contribution of inherent stepping in upward positive leaders to the current pulses that we report here. Future observations that will include broadband electric field measurements and high speed (>100,000 frames per second) video observations in conjunction with current measurements should help separate the two likely causes of these UUL current pulses.

The UUL background current amplitude is likely related to the length of developing upward leader which in turn depends upon the approaching downward negative leader electric field. For three of our UULs background currents and pulse amplitudes increased, and interpulse intervals were shorter at later times during the UULs' development phases (see Fig. 6). We hypothesized that these UULs likely developed to be of significant lengths (perhaps several tens to 100 m). In these cases, a downward leader branch and the UUL approached each other closely, perhaps getting within 100 m or so each other, just prior to another branch of the downward leader attaching to ground via a UCL in the tower's proximity. For three other UULs in our dataset the background currents and pulse amplitudes did not increase, and interpulse intervals did not change significantly between early and later times in their development phase. It is possible that these UULs were likely relatively stagnant (from the perspective of their length). High-speed video observations of UULs in conjunction with their current measurements are needed to confirm these speculations.

Declaration of Competing Interest

The authors declare that they have no known competing financial interests or personal relationships that could have appeared to influence the work reported in this paper.

Acknowledgements

The authors would like to acknowledge funding from the U.S.

National Science Foundation Award 1934066 and U.S. Air Force contract FA252117P0079. Data used in this paper is available by contacting the first author (anag@fit.edu).

References

- Becerra, M., Cooray, V., 2006a. A self-consistent upward leader propagation model. J. Phys. D. Appl. Phys. 39, 3708–3715. https://doi.org/10.1088/0022-3727/39/16/028
- Becerra, M., Cooray, V., 2006b. Time dependent evaluation of the lightning upward connecting leader inception. J. Phys. D. Appl. Phys. 39, 4695–4702. https://doi.org/ 10.1088/0022-3727/39/21/029.
- Berger, K., Anderson, R.B., Kröninger, H., 1975. Parameters of lightning flashes. CIGRE Electra 41, 23–37.
- Biagi, C.J., Jordan, D.M., Uman, M.A., Hill, J.D., Rakov, V.A., Dwyer, J., 2010. Observations of stepping mechanisms in a rocket-and wire triggered lightning flash. J. Geophys. Res. 115, D23215 https://doi.org/10.1029/2010JD014616.
- Biagi, C.J., Uman, M.A., Hill, J.D., Jordan, D.M., 2011. Observations of the initial, upward-propagating, positive leader steps in a rocket-and-wire triggered lightning discharge. Geophys. Res. Lett. 38, L24809 https://doi.org/10.1029/2011GL049944.
- Cummins, K.L., Krider, E.P., Olbinski, M., Holle, R.L., 2018. A case study of lightning attachment to flat ground showing multiple unconnected upward leaders. Atmos. Res. 202, 169–174. https://doi.org/10.1016/j.atmosres.2017.11.007.
- Cummins, K.L., Nag, A., Plaisir, M.N., Austin, M., Crawford, D., Wilson, J., Brown, R.G., Noggle, C., Rassoul, H.K., 2019. Characteristics of upward leader currents measured at the KSC industrial area tower. In: AGU 2019 Fall Meeting. American Geophysical Union, San Fransisco, p. #AE12A-01.
- Hill, J., Mata, C., Roeder, W., 2016. Evaluation of the performance characteristics of MERLIN and NLDN based on two years of ground-truth data from Kennedy Space Center/Cape Canaveral Air Force Station, Florida. In: 24th International Lightning Detection Conference (ILDC)International Lightning Detection Conference. https://nam03.safelinks.protection.outlook.com/?url=https%3A%2F% 2Fmy.vaisala.net%2FVaisala%2520Documents%2FScientific%2520papers%2F2 016%2520ILDC%2520ILMC%2FJonathan%2520Hill%2520et%2520al.%2520Eval uation%25200f%2520ILMC%2FJOnathan%2520Characteristics%2520of%2520MERLIN%2520and%2520NLDN.pdf&data=04%7C01%7Cj.bakthavachalam.1% 40elsevier.com%7Cfccbfd74796e48c2cb9008d8b18af4f2%7C9274ee3f94254109a2 7f9fb15c10675d%7C0%7C0%7C6374545581122772138%7CUnknown%7CTWFp bGZsb3d8eyJWIjoiMC4wLjAwMDAiLCJQIjoiV2luMZilLCJBTiIf6lk1ha Wwil.CJXVCI6Mn0%3D%7C1000&sdata=wmzn5nHJ2RaihPvISTike5TQ710Yztq W1%2F0siP8%2BOT4%3D&reserved=0 (San Diego).
- Jiang, R., Qie, X., Wang, C., Yang, J., 2013. Propagating features of upward positive leaders in the initial stage of rocket-triggered lightning. Atmos. Res. 129–130, 90–96. https://doi.org/10.1016/j.atmosres.2012.09.005.
- Jiang, R., Qie, X., Wang, Z., Zhang, H., Lu, G., Sun, Z., Liu, M., Li, X., 2015. Characteristics of lightning leader propagation and ground attachment. J. Geophys. Res. Atmos. 120 https://doi.org/10.1002/2015JD023519.
- Krider, E.P., Weidman, C.D., Noggle, R.C., 1977. The electric fields produced by lightning stepped leaders. J. Geophys. Res. 82, 951–960. https://doi.org/10.1029/ ic082i006p00951
- Lu, W., Chen, L., Ma, Y., Rakov, V.A., Gao, Y., Zhang, Yang, Yin, Q., Zhang, Yijun, 2013. Lightning attachment process involving connection of the downward negative leader to the lateral surface of the upward connecting leader. Geophys. Res. Lett. 40, 5531–5535. https://doi.org/10.1002/2013GL058060.
- McEachron, K.B., 1939. Lightning to the empire state building. J. Frankl. Inst. 227, 149–217. https://doi.org/10.1016/S0016-0032(39)90397-2.
- Miki, T., Saito, M., Shindo, T., Ishii, M., 2019. Current observation results of downward negative flashes at Tokyo Skytree From 2012 to 2018. IEEE Trans. Electromagn. Compat. 61, 663–673. https://doi.org/10.1109/TEMC.2019.2910319.
- Pu, Y., Jiang, R., Qie, X., Liu, M., Zhang, H., Fan, Y., Wu, X., 2017. Upward negative leaders in positive triggered lightning: Stepping and branching in the initial stage. Geophys. Res. Lett. 44, 7029–7035. https://doi.org/10.1002/2017GL074228.
- Qie, X.S., Yuan, S.F., Zhang, H.B., Jiang, R.B., Wu, Z.J., Liu, M.Y., et al., 2019. Propagation of positive, negative, and recoil leaders in upward lightning flashes. Earth Planet. Phys. 3 (2), 102–110. https://doi.org/10.26464/epp2019014.

- Rakov, V.A., Uman, M.A., 2003. Lightning: Physics and Effects. Cambridge Univ. Press, New York. https://nam03.safelinks.protection.outlook.com/?url=https%3A%2F% 2Fdoi.org%2F10.1017%2FCB09781107340886&data=04%7C01%7Cj.bakthavach alam.1%40elsevier.com%7Cfccbfd74796e48c2cb9008d8b18af4f2%7C9274ee 3f94254109a27f9fb15c10675d%7C0%7C0%7C637454558122772138% 7CUnknown%7CTWFpbGZsb3d8e yJWIjoiMC4wLjAwMDAiLCJQIjoiV2luMzliLCJBTiI6Ik1haWwiLCJXVCI6Mn0%3D% 7C1000&sdata=cLsJBcy16RXcvaipy1ZBmFlrB6PY6t8OOI5Xto4%2BnBo%3D&reservad=0
- Roeder, W.P., Saul, J., 2017. The new mesoscale eastern range lightning information system. In: 18th Conference on Aviation Range and Aerospace Meteorology. American Meteorological Society Annual Meeting, Seattle, Washington. https://nam.03.safelinks.protection.outlook.com/?url=https%3A%2F%2Fams.confex.com% 2Fams%2F97Annual%2Fwebprogram%2FPaper306080.html&data=04%7C01% 7Cj.bakthavachalam.1%40elsevier.com%7Cfccbfd74796e48c2cb9008d8b18af4f2% 7C9274ee3f94254109a27f9fb15c10675d%7C0%7C0%7C637454558122772138% 7CUnknown%7CTWFpbGZsb3d8e yJWIjoiMC4wLjAwMDAiLCJQIjoiV2luMzIiLCJBTiI6Ik1haWwiLCJXVCI6Mn0%3D% 7C1000&sdata=BZ5c%2B87CCu32%2BSfPOBZIWzebociuqbuFx6BBh8Y39Pc% 3D&reserved=0.
- Schoene, J., Uman, M.A., Rakov, V.A., Jerauld, J., Hanley, B.D., Rambo, K.J., Howard, J., DeCarlo, B., 2008. Experimental study of lightning-induced currents in a buried loop conductor and a grounded vertical conductor. IEEE Trans. Electromagn. Compat. 50, 110–117. https://doi.org/10.1109/TEMC.2007.911927.
- Srivastava, A., Jiang, R., Yuan, S., Qie, X., Wang, D., Zhang, H., Sun, Z., Liu, M., 2019. Intermittent Propagation of Upward positive Leader Connecting a Downward negative Leader in a negative Cloud-to-Ground Lightning. J. Geophys. Res. Atmos. 124, 13763–13776. https://doi.org/10.1029/2019JD031148.
- Stolzenburg, M., Marshall, T.C., Karunarathne, S., Orville, R.E., 2018. Length estimations of presumed upward connecting leaders in lightning flashes to flat water and flat ground. Atmos. Res. 211, 85–94. https://doi.org/10.1016/j.atmosres.2018.04.020.
- Takami, J., Okabe, S., 2007. Observational results of lightning current on transmission towers. IEEE Trans. Power Deliv. 22, 547–556. https://doi.org/10.1109/ TPWRD.2006.883006.
- Visacro, S., Soares, A., Schroeder, M.A.O., Cherchiglia, L.C.L., de Sousa, V.J., 2004. Statistical analysis of lightning current parameters: Measurements at Morro do Cachimbo station. J. Geophys. Res. Atmos. 109 https://doi.org/10.1029/ 2003id003662.
- Visacro, S., Murta Vale, M.H., Correa, G., Teixeira, A., 2010. Early phase of lightning currents measured in a short tower associated with direct and nearby lightning strikes. J. Geophys. Res. Atmos. 115 https://doi.org/10.1029/2010JD014097.
- Visacro, S., Mesquita, C.R., De Conti, A., Silveira, F.H., 2012. Updated statistics of lightning currents measured at Morro do Cachimbo Station. Atmos. Res. 117, 55–63. https://doi.org/10.1016/j.atmosres.2011.07.010.
- Visacro, S., Guimaraes, M., Murta Vale, M.H., 2017a. Features of upward positive leaders initiated from towers in natural cloud-to-ground lightning based on simultaneous high-speed videos, measured currents, and electric fields. J. Geophys. Res. Atmos. 122. 12.786–12.800. https://doi.org/10.1002/2017JD027016.
- Visacro, S., Guimaraes, M., Murta Vale, M.H., 2017b. Striking distance determined from high-speed videos and measured currents in negative cloud-to-ground lightning.

 J. Geophys. Res. Atmos. 122, 13,356–13,369. https://doi.org/10.1002/2017JD027354.
- Wang, Z., Qie, X., Jiang, R., Wang, C., Lu, G., Sun, Z., Liu, M., Pu, Y., 2016. High-speed video observation of stepwise propagation of a natural upward positive leader. J. Geophys. Res. Atmos. 121, 14307–14315. https://doi.org/10.1002/ 2016.JD025605.
- Wang, X., Wang, D., He, J., Takagi, N., 2020. A comparative study on the discontinuous luminosities of two upward lightning leaders with opposite polarities. J. Geophys. Res. Atmos. 125 https://doi.org/10.1029/2020JD032533.
- Res. Atmos. 125 https://doi.org/10.1029/2020JD032533.

 Zhou, H., Diendorfer, G., Thottappillil, R., Pichler, H., Mair, M., 2014. The influence of meteorological conditions on upward lightning initiation at the Gaisberg Tower. In: 2014 International Conference on Lightning Protection (ICLP), Shanghai, China, pp. 1162–1165. https://doi.org/10.1109/ICLP.2014.6973303.